

Quantitative determination of the $O(^3P)$ density via visible cavity-enhanced spectroscopy

Manish Gupta,^{a)} Thomas Owano, Douglas Baer, and Anthony O'Keefe
 Los Gatos Research, 67 East Evelyn Avenue, Suite 3, Mountain View, California 94041

(Received 13 September 2006; accepted 11 November 2006; published online 15 December 2006)

A simple method has been developed to quantitatively measure the ground state oxygen atom, $O(^3P)$, density. The technique exploits cavity-enhanced spectroscopy to probe the relatively weak $O(^1D) \leftarrow O(^3P_1)$ transition near 636 nm. $O(^3P_1)$ densities of approximately 3.4×10^{14} at./cm³ were measured in an inductively coupled plasma produced within a high-finesse optical cavity, and a minimum detectable atom state density of 1.3×10^{12} at./cm³ was determined. The absorption profile yielded a translational temperature of 453 K. The technique can be readily extended to other atomic species. © 2006 American Institute of Physics. [DOI: 10.1063/1.2408655]

Oxygen atoms play a vital role in many industrial plasma processes including chamber cleaning and polymer etching. They are also a key component of the upper atmosphere and contribute to the well-known nightglow phenomenon. In order to better understand and model these processes, a quantitative measure of O atom density is required. Moreover, since in many of these instances the majority of the atom density is in the ground electronic state, a direct measurement of $O(^3P)$ is needed.

Previous techniques have included downstream titration, normalized oxygen atom emission, laser-induced fluorescence, tunable diode laser absorption spectroscopy of excited oxygen atoms, and vacuum ultraviolet atomic resonance absorption spectroscopy.^{1,2} In general, most of these methodologies require extensive equipment, calibration, and the correlation of several measured species. Notable exceptions include recent work involving vacuum ultraviolet laser absorption spectroscopy³ and cavity ringdown spectroscopy⁴ which provide direct quantification of $O(^3P)$, but are complicated by the need for extensive experimental apparatus.

In this letter, we present a simple alternative that involves using readily available visible diode lasers near 630 nm to probe the absolute density of $O(^3P)$ via the $O(^1D) \leftarrow O(^3P)$ transitions. A high-finesse optical cavity is utilized to compensate for the small absorption cross section of the transition.

The oxygen atom has 11 distinct electron configurations below its ionization level, ranging from the ground state (3P) to a high-lying 3D state near 97 488 cm⁻¹. Amongst these levels there are several "allowed" optical transitions which follow the traditional selection rules. In the example noted above, the 3P ground state was probed via the $^3S^0 \leftarrow ^3P$ transition near 130 nm that has Einstein A coefficients⁵ ranging $A=0.676-3.41 \times 10^8$ s⁻¹. Likewise, excited O atoms have been probed via the $^5P_3 \leftarrow ^5S_2^0$ and $^3P_2 \leftarrow ^3S_0^0$ transitions⁶ near 777 and 845 nm, respectively, with $A=3.7 \times 10^7$ s⁻¹ and $A=3.22 \times 10^7$ s⁻¹. Although experimentally preferential due to the availability of visible diode lasers and associated hardware, the low-lying electronic states of the O atom (1D and 1S) are not allowed transitions from the 3P ground state. For example, the $^1D \leftarrow ^3P_1$ transition employed in this work has

an Einstein A coefficient⁷ of only $A=1.82 \times 10^{-3}$ s⁻¹. This very weak absorption strength prohibits the use of traditional visible laser absorption spectroscopy.

Both intracavity laser spectroscopy⁸ and cavity ringdown spectroscopy⁴ have been employed to circumvent this limitation. For atom densities exceeding 10^{14} at./cm³, Teslja and Dagdigian measured the $^1D \leftarrow ^3P_2$ transition of atomic oxygen near 630.03 nm and verified that the optical determination was consistent with the results obtained by nitrogen dioxide chemical titration. However, the bandwidth of the pulsed dye laser used in this experiment was substantially larger than the width of the $O(^3P_2)$ spectral feature, making it difficult to determine a translational temperature from the measurements.

In this study, off-axis integrated cavity output spectroscopy⁹ (off-axis ICOS) is employed to make the diagnostic more compact, sensitive, and robust. In off-axis ICOS, a narrow-linewidth (<10 MHz typical), cw diode laser is coupled into a high-finesse optical cavity composed of two highly reflective mirrors ($R > 99.95\%$ typical) which increase the effective optical path length by a factor of $(1-R)^{-1}$ (>2000 typical). By coupling this path length enhancement with an off-axis alignment scheme optimized to reduce transmission noise due to laser interferences, very weak absorption signals (< 10^{-10} cm⁻¹ typical) can be readily observed. This extraordinary sensitivity makes "forbidden" optical transitions readily accessible. Moreover, by rapidly switching off the laser and measuring the rate at which light decays out of the cavity (e.g., cavity ringdown measurement), the effective optical path length can be precisely measured, obviating the need for any external calibration.

The experimental setup is shown in Fig. 1. The 93.7 cm long optical cavity consisted of a 69.9 cm long center quartz tube bounded by two adjustable bellow mounts containing the highly reflective cavity mirrors ($R=99.963\%$). A 635 nm Fabry-Pérot diode laser (Thorlabs DL5038-021, 30 mW) mounted into a standard TO-5 laser mount to provide temperature control and collimation was directed into the cavity in an off-axis fashion. Light transmitting through the cavity was focused by an aspheric lens onto highly amplified, low-noise silicon detector. The center laser frequency was 636.43 ± 0.1 nm as determined by a HeNe-calibrated monochromator. The laser was scanned 0.05 nm (40 GHz as de-

^{a)} Author to whom correspondence should be addressed; electronic mail: m.gupta@lgrinc.com

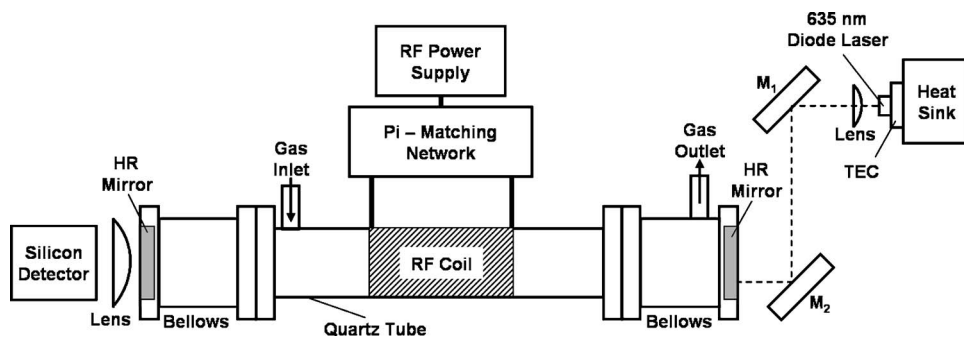


FIG. 1. Experimental setup. The oxygen atoms are generated within a high-finesse optical cavity via a RF-ICP. A temperature-controlled Fabry-Pérot diode laser near 636 nm is coupled into the cavity in an off-axis fashion, and the transmitted light is focused onto an amplified silicon detector. The laser is scanned in frequency and the cavity-enhanced absorption spectrum of $O(^3P_1)$ is measured directly.

terminated by an external solid étalon) at 25 Hz by ramping its current from 94 to 102 mA. Approximately 1000 such scans were averaged to yield the data presented below.

Due to their highly reactive nature, oxygen atoms were generated inside the quartz portion of the optical cavity via an *in situ* radio frequency inductively coupled plasma (rf-ICP) operating at 13.56 MHz. An oil-free scroll pump was used to flow a 10% O_2/He mixture through the cavity at a rate of approximately 3000 SCCM (SCCM denotes cubic centimeter per minute at STP). Typical operating pressures ranged from 10 to 40 Torr and were actively controlled using an upstream pressure controller to prevent density fluctuations. The rf power coupled into the plasma was varied between 0 and 300 W and the reflected power was minimized via a pi-matching network. At the lower pressures and high powers, the plasma was observed to fill the quartz tube without extending into the metal bellows, and oxygen atom generation was confirmed by emission.

The effective cavity path length was determined to be 2544 m by cavity ringdown measurements ($\tau = 8.48 \pm 0.01 \mu s$). Since the plasma does not extend into the metal bellows, the effective path length through the plasma is 1897 m.

The cavity-enhanced absorption spectrum of $O(^3P_1)$ fits well to a single Voigt profile and is shown in Fig. 2 at a pressure of 20 Torr and rf power at 275 W. The absorption is only present when the plasma is activated indicating that it is due to oxygen atoms, helium atoms, or molecules (e.g., oxygen or trace water) at an elevated temperature. At the absorbing wavelength, there are no helium atom transitions. Like-

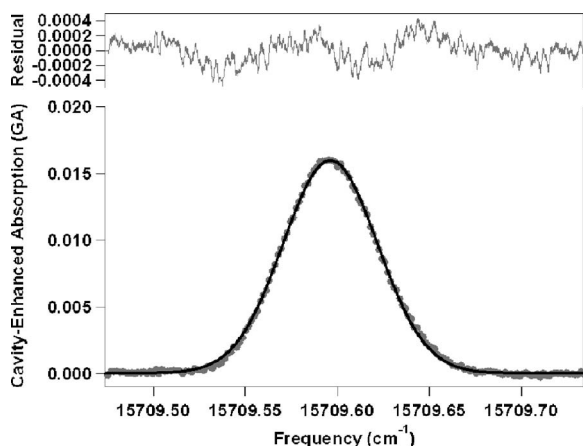


FIG. 2. Measured cavity-enhanced absorption spectrum of $O(^3P_1)$ near 636 nm with a signal to noise ratio exceeding 260:1. The measured Doppler width of 0.05984 cm^{-1} corresponds to a translational temperature of 453 K. The integrated area of the feature yields an atom density of $3.4 \times 10^{14} \text{ at./cm}^3$.

wise, spectral simulations show that, at elevated temperatures, trace water absorptions become even weaker than at room temperature, making them immeasurable at the given conditions. The only other potential absorbing transition near this wavelength region is the $^3Q(34)$ line of the (2,0) band of the $b^1\Sigma_g^- \leftarrow X^3\Sigma_g^-$ transition in molecular oxygen.¹⁰ However, at the plasma temperature (described below) the anticipated absorption is only 3×10^{-5} , much smaller than the measured absorption of 0.016.

The Doppler width of the measured transition is $0.05984 \pm 0.00019 \text{ cm}^{-1}$, indicating a translational temperature of $453 \pm 10 \text{ K}$. An independent plasma temperature of 326 K was determined by measuring the $Q(13)$ line of the (0,0) band of the $a \leftarrow X$ transition in molecular oxygen near 1269.23 nm. The discrepancy is attributed to colder oxygen molecules (e.g., 300 K) inside the metal bellows and outside of the quartz region in which oxygen atoms are present. The Lorentzian width of the transition is only $0.00089 \pm 0.00018 \text{ cm}^{-1}$, indicating negligible broadening due to the background gas.

The integrated area of measured absorption is $0.001046 \pm 0.000011 \text{ cm}^{-1}$. Taking into account an effective path length of 1897 m and integrated absorption cross section of $S_{\text{int}} = 1.63 \times 10^{-23} \text{ cm}^2/\text{at.}$ determined from an Einstein A coefficient⁷ of $A = 1.82 \times 10^{-3} \text{ s}^{-1}$, this area corresponds to an atomic state density of $3.38 \times 10^{14} \text{ at./cm}^3$. Given that the measurement signal-to-noise ratio (peak signal to rms noise) is 260:1, the minimum detectable atomic oxygen state density is $1.3 \times 10^{12} \text{ at./cm}^3$. By using mirrors of higher reflectivity and better filtering rf noise due to plasma generation, previous results suggest that the minimum detectable density can be readily reduced by an order of magnitude. It is important to note that the measured atomic density is path integrated through the plasma and does not provide spatial information.

Visible cavity-enhanced absorption spectroscopy has been used to quantify ground-state oxygen atom density in a rf-ICP. Unlike other current techniques, the methodology provides absolute densities and translational temperatures without calibration in a simple experimental implementation. In addition to $O(^3P)$, off-axis ICOS of forbidden atomic transitions will enable direct quantification of other atomic species and their excited states.

Funding for Los Gatos Research Inc. (LGR) was provided through the MDA SBIR program (Grant No. FA8651-06-M-0137).

¹J. P. Booth, O. Joubert, J. Pelletier, and N. Sadeghi, J. Appl. Phys. **69**, 618 (1991).

²H. Nagai, M. Hiramatsu, M. Hori, and T. Goto, Rev. Sci. Instrum. **74**,

3453 (2003), and references therein.

³K. Takeda, Y. Kubota, Y. Matsumi, and M. Hori, 2005 Proc. Int. Conf. Phenom. Ionized Gases 08-397, available at <http://www.icipig2005.nl/cd/D:/pdf/08-397.pdf>

⁴A. Teslja and P. J. Dagdigian, Chem. Phys. Lett. **400**, 374 (2004).

⁵W. C. Martin, J. R. Fuhr, D. E. Kelleher, A. Musgrove, J. Sugar, W. L. Wiese, P. J. Mohr, and K. Olsen, NIST Atomic Spectra Database, version 2.0 (1999); available online at <http://physics.nist.gov/asd2>, 2006.

⁶E. Biemont and C. J. Zeippen, Astron. Astrophys. **265**, 850 (1992).

⁷K. L. Baluja and C. J. Zeippen, J. Phys. B **21**, 1455 (1988).

⁸S. J. Harris and A. M. Weiner, Opt. Lett. **6**, 434 (1981).

⁹D. S. Baer, J. B. Paul, M. Gupta, and A. O'Keefe, Appl. Phys. B: Lasers Opt. **75**, 261 (2002).

¹⁰L. S. Rothman, D. Jacquemart, A. Barbe, D. Benner, M. Birk, L. R. Brown, M. R. Carleer, C. Chackerian, K. Chance, L. H. Coudert, V. Dana, V. M. Devi, J.-M. Flaud, R. R. Gamache, A. Goldman, J.-M. Hartmann, K. W. Jucks, A. G. Maki, J.-Y. Mandin, S. T. Massie, J. Orphal, A. Perrin, C. P. Rinsland, M. A. H. Smith, J. Tennyson, R. N. Tolchenov, R. A. Toth, J. V. Auwera, P. Varanasi, and G. Wagner, J. Quant. Spectrosc. Radiat. Transf. **96**, 139 (2005).